Hindawi
Shock and Vibration
Volume 2018, Article ID 4708730, 14 pages
https://doi.org/10.1155/2018/4708730

Research Article

Unbalanced Vibration Identification of Tangential Threshing Cylinder Induced by Rice Threshing Process

Zhong Tang, Haotian Zhang, and Yuepeng Zhou

School of Agricultural Equipment Engineering, Jiangsu University, Zhenjiang, Jiangsu 212013, China

Correspondence should be addressed to Zhong Tang; tangzhong2012@126.com

Received 27 February 2018; Accepted 16 April 2018; Published 27 May 2018

Academic Editor: Mickaël Lallart

Unbalanced vibration of tangential threshing cylinder increased the grain loss, shortened service life of the cylinder, and resulted in structural resonance during the rice threshing process. In this paper, the vibration amplitude and frequency of tangential threshing cylinder shaft were tested, and the vibration state of tangential threshing cylinder was identified. The restricted and working modalities of tangential threshing cylinder were solved by ANSYS software. Then, by comparing the resonance phenomenon between the inherent constraint frequency and the rotation speed frequency, the shaft vibration under the idle condition of tangential threshing cylinder was tested and analyzed. According to the axial vibration and axial trajectory of the cylinder, the inherent properties and characteristics of unbalanced vibration were revealed. Test results showed that when the tangential threshing cylinder was at idling and no-load state, the amplitude of vibration in the feed direction of straw flow was −0.049~0.060 mm, and the average vibration amplitude was 0.013 mm. As rice flowed along the tangential threshing cylinder, the vibration amplitude slightly increased. The trend and phase of each trajectory were similar, although the amplitude of each trajectory was different. The tangential threshing cylinder axis trajectory was flat oval. Unbalanced vibration was induced by the rice stalks in the concave gap.

1. Introduction

During the threshing process of rice, the straw was propelled toward the threshing bar along the circumferential portion of the tangential threshing cylinder. And straws were partially loaded on the tangential threshing cylinder. Unbalanced vibration was induced by partial load on tangential threshing cylinder [1]. Unbalanced vibration of tangential threshing cylinder resulted in increased grain loss, shortened cylinder life, and resonance of structure during the process of rice threshing [2]. Therefore, it was very important to deal with the vibration problem caused by rice threshing.

During harvesting operation, excessive vibrations of the combine harvester can affect working precision and driver's comfort [3, 4]. Tomczyk and Kowalczyk proposed the issue of shaping the structure quality of combine harvester and analyzed the observed types and processes of harvester's structure [5]. In order to reduce the vibration of combine harvester, vibration of cutter bar driver was a research hotspot. Fukushima et al. revealed that the harmonic frequency components varied with an increasing width of the interspace, although the highest harmonic frequency in the simulation was three times for the crank wheel rotation frequency [6]. Chuan-Udom developed 3 types of new cutter bar drivers to reduce the vibration of rice combine harvester [7]. There was a considerable amount of research studies focusing on cutter bar. And many solutions for header vibration were also proposed. When vibration of cutter bar was reduced, the vibration of rice threshing process was more obvious and serious. Gao et al. tested the vibration of crawler-type combine harvester under field harvesting conditions, indicating that significant vibration was caused by the harvesting state [8].

In order to reduce the vibration induced by harvesting state, the balanced tangential threshing cylinder is required to be in a dynamic threshing process. Polushkin et al. developed a specialized system for the preresonant balancing of universal joints [9]. That model must be based on vector coefficients characterizing the influence of imbalances. In order to obtain the relationship between the inherent modal

characteristics and the vibration, Zhou et al. investigated the cylinder modal analysis of threshing and verified the reliability of grain threshing cylinder structure by ANSYS [10]. The modeling of a flexible rotor on magnetorheological squeeze film damper was carried out by Zapomel et al., focusing on determining the distribution of lubrication layer and damping force calculation [11]. The above results show that vibration frequency, threshing cylinder mode, and threshing load are important factors in vibration.

Nonlinear vibration occurred due to the locations of the harvesting state. Vibration levels of different harvesters were significantly different [12–14]. In order to reduce the vibration of the combine harvester threshing cylinder under the normal load, the vibration characteristics of five flap type portable harvesters used for olive harvesting at both idling and full load conditions were measured and evaluated [15]. The theory various frequencies of vibration rate and mode shape also were analyzed by ANSYS Workbench modal [16]. Although the location arrangements were similar, the vibration characteristics were different [17]. Hagiwara et al. presented a way of analyzing the vibration of a rotor shaft system coupled with flexible impellers based on the transfer method [18]. This calculation of the vibration response of a rotor shaft system could develop the unbalance response of a rotor. Most relevant vibration property of the combine cutting platform was experimental assessment by frequency domain decomposition technique. The frequency resolution of acceleration could be measured in a time series, and the vibration characteristics of each frequency component could be examined. Available frequency domain decomposition techniques can provide very accurate natural frequency and mode shapes [19]. Thus far little research and result on the measurement as well as evaluation and modeling of vibration about rice threshing process have been published. With the rationalization of structural design of rice combine harvester, the header and engine with greater vibration are effectively controlled. However, the vibration of the threshing cylinder in the rice threshing process becomes particularly prominent. The vibrations induced by rice threshing process resulted in a violent bouncing of the transmission chain. It also increased the grain loss, shortened service life of the cylinder, and resulted in structural resonance.

In this paper, the tangential thresholding cylinder restricted and working modalities were solved based on the software ANSYS Workbench. By comparing the resonance phenomenon between the inherent constraint frequency and the speed, the shaft vibration under the idle condition of the threshing cylinder was tested and analyzed. According to the axial vibration and axial trajectory of the threshing cylinder, the inherent properties and characteristics of the unbalanced vibration were revealed.

2. Material and Methods

2.1. Unbalanced Vibration Test Bench in Rice Threshing. Tangential threshing cylinder is an important threshing device of rice combine harvester. In the rice threshing process, there was only one-third circumferential surface of cylinder contacted with rice straw. Therefore, there was eccentric load acting on tangential threshing cylinder [20]. This eccentric load acting was central angle about 100° on the section of threshing cylinder. Figure 1 showed the straw flow in the tangential threshing cylinder and the eccentric load of the threshing cylinder.

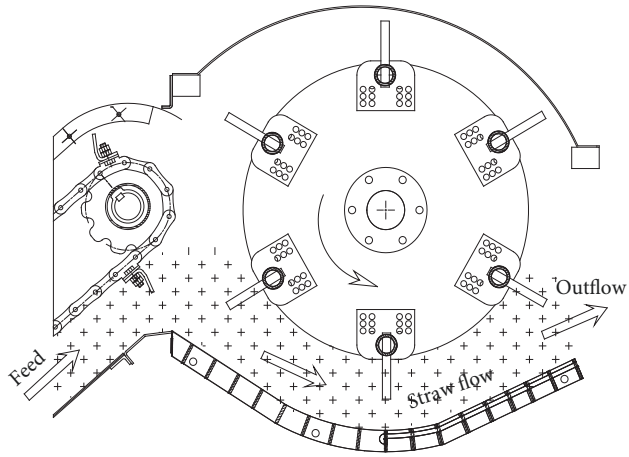

Figure 1: Rice straw flow and eccentric load in tangential threshing process.

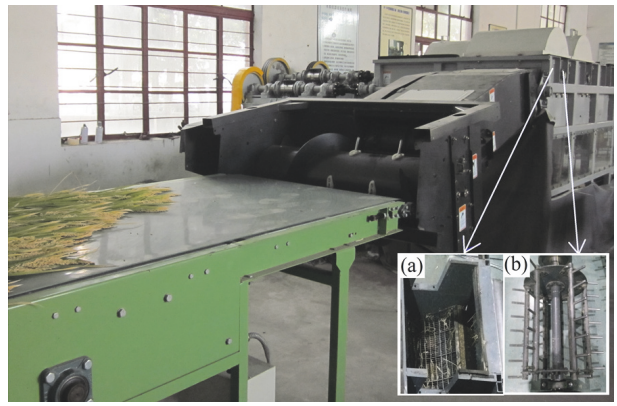

(a) Grid concave, (b) Tangential threshing cylinder

Figure 2: Tangential threshing cylinder test bench.

In order to identify the unbalanced vibration caused by the threshing process of rice, the threshing test of rice was carried out on tangential threshing cylinder test bench. The test bench was composed of conveying platform, feeding screw, conveying chute, grid concave, tangential threshing cylinder, and other components [21]. Tangential threshing cylinder test bench was shown in Figure 2. The tangential threshing cylinder diameter and length were 525 mm and 550 mm, respectively. The rotation speed was 700 rpm. During the rice threshing process, the straw was propelled toward the threshing bar along the circumferential portion of the tangential threshing cylinder. And straws partially were loaded on the tangential threshing cylinder. The unbalanced vibration was induced by partial load on tangential threshing cylinder. Structure and principle of tangential threshing cylinder were also studied by Miu and Kutzbach [1].

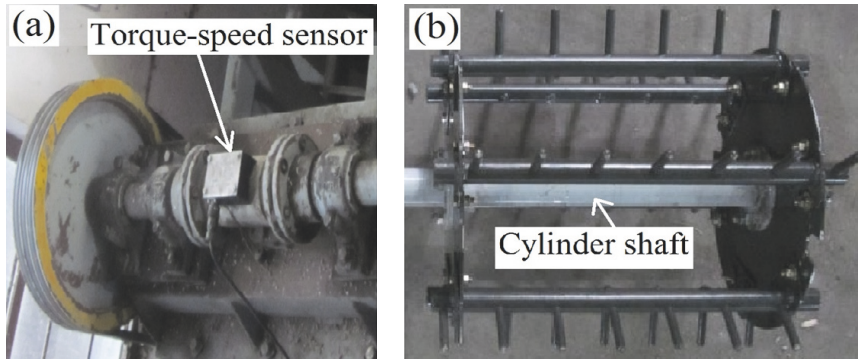

(a) Drive and torque test structure (b) Tangential threshing cylinder and shaft

Figure 3: Drive and torque test structure of tangential threshing cylinder.

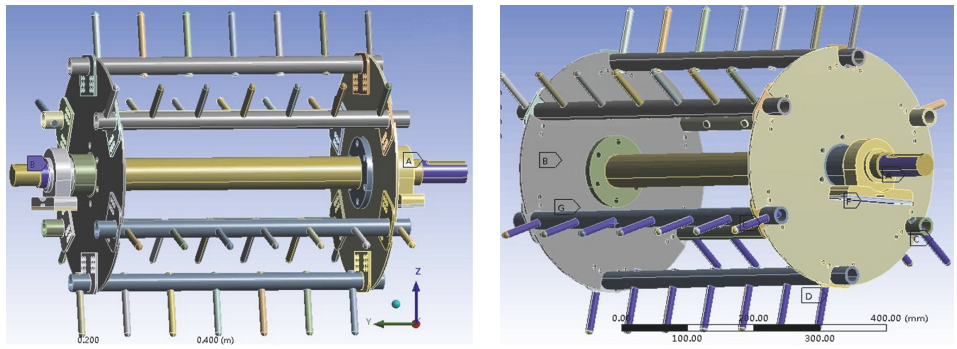

(a) Restricted modality by bearing (b) Working modality by threshing bars

Figure 4: Restricted and working modalities analysis of tangential threshing cylinder.

2.2. Torque and Speed Test in Rice Threshing Process. The tangential threshing cylinder was driven by frequency conversion motor. The power was input by a belt reel. HAD-CYB-803S torque sensor (Beijing Westzh M & E Technology Co., Ltd., China) and two bearing seats were installed between belt reel and tangential threshing cylinder. The drive and torque test structure of tangential threshing cylinder was shown in Figure 3.

During the threshing process, the torque-speed sensor measured the torque value and speed of tangential threshing cylinder shaft. The measurement accuracy of torque and speed sensor was 0.25% full scale and frequency response time of 100 μs.

2.3. Restricted and Working Modalities of Tangential Threshing Cylinder. Modal of tangential threshing cylinder had inherent attributes and traits. There were two types of modalities for the tangential threshing cylinder [22, 23]. The first one was restricted modalities, which was bound by the both ends of the drive shaft in bearings. The second one was working modalities, which was compound modalities. Modal was determined by the tangential threshing cylinder and rice straw interaction. When the rotation frequency was the same as the natural frequency of tangential threshing cylinder, the barrel would send resonance and the shaft vibration would increase dramatically. The restricted modality of tangential threshing cylinder was bound by both ends of the drive shaft in bearings. There were only two constraints between the shaft and bearing.

ANSYS was widely used in many industries, it also used to describe and analyze the structural state [24]. The 3D model of tangential threshing cylinder was developed by Pro/E software and saved as STEP format. Then the 3D model was imported into ANSYS Workbench. Then the restricted modality developed by ANSYS was shown in Figure 4(a). There were two cylindrical constraint positions at both axial ends, which were Point A and Point B. Tangential threshing cylinder could rotate only with the cylindrical constraint positions A and B axis.

When the tangential threshing cylinder was threshing rice, the threshing bars were bound by the rice stems. And the modality of tangential threshing cylinder was changed by restrictions. The working modality restricted by threshing bars and bearings was shown in Figure 4(b). There were five constraint positions. Both axial ends of tangential threshing cylinder were cylindrical constraint positions shown as Point A and Point B. Three rows threshing bars were fixed constraints shown as Point C, Point D, and Point E. Bearings at both ends were in a fixed restraint state.

In order to facilitate the determination of modal and vibrational directions, set up a coordinate system on the tangential threshing cylinder structure. X direction represented

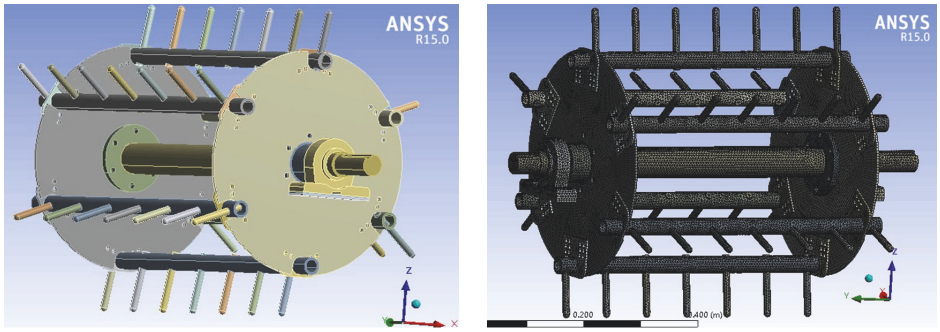

(a) Imported model (b) Mesh model

Figure 5: Analysis model of tangential threshing cylinder.

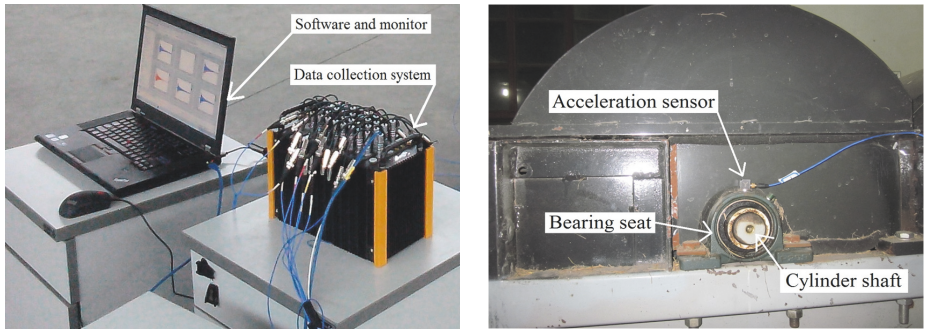

(a) Dynamic signal acquisition instrument (b) Acceleration sensor on bearing seat

Figure 6: Bearing seat vibration test of tangential threshing cylinder.

the feed straw flow direction, which was the front and back direction. Y direction represented the cylinder axis, which was in left and right direction. Z direction represented the cylinder axis, which was in up and down direction. The coordinate system was shown in Figure 5(a). The restricted and working modalities were analyzed by ANSYS software. The restricted and working modalities were used to compare with the speed and other exciting frequency.

Meshing was an important step in modal analysis by ANSYS software [25]. Automatic meshing method was adopted, which automatically detected the entities. Then the swept method was used to divide the hexahedral grids into entities that can be swept, and the coordination slicing algorithm was used to divide the tetrahedron grids into entities that cannot be swept. Because the tangential threshing cylinder has a minimum structural thickness of 4 mm, the grid size was 4 mm and the meshing result was shown in Figure 5(b).

2.4. Vibration Test in Rice Threshing Process. The vibration signal acquisition system and signal analysis and processing system were composed, shown in Figure 6(a). The signal acquisition system and dynamic signal acquisition instrument were produced by Chinese Donghua testing company (DH5902 dynamic signal acquisition instrument). The signal acquisition systems collected the electrical signal of acceleration test point on tangential threshing cylinder with 3 kinds of conditions. Signal acquisition system used the United States of America (PCB) 356A16 type three acceleration sensors. Vibration signal was tested by 356A16 type acceleration sensor. The vibration of tangential threshing cylinder was tested at the bearing seat. Vibration test of acceleration sensor on bearing seat was shown in Figure 6(b).

Test performance parameters of Chinese Donghua testing company's DH5902 dynamic signal acquisition instrument were shown in Table 1.

2.5. Unbalanced Vibration Test Methods. Freshly cut rice (72 kg) was placed on a 12 m × 1 m conveyer belt at the liner speed of 1 m/s (with constantly feeding rate of 6 kg/s). The unbalanced vibration was tested at two states of idling: state of no-load and load state of rice threshing process [26]. The unbalanced vibrations of bearing seat were used to represent the vibration of tangential threshing cylinder. The complete parameter estimation procedure and the results of all tests were repeated five times to reduce the impact of random influence on choice of validation set. The mean data were analyzed statistically. Then mean results were compared by least significant difference (LSD) post hoc test at the 5% significance level ($p < 0.05$).

Table 1: Performance parameters of vibration test instruments.

Equipment name	Performance index	Parameter values	Manufacturer
Three-direction acceleration sensor of 356A16	Sensitivity	100 mV/g	American voltage Company (PCB)
	Frequency response	0.3~6 KHz	
	Range	±50 g pk	
	Lateral sensitivity	<5%	
Dynamic signal acquisition instrument of DH5902	Channel	32	Chinese Donghua testing company
	Sampling bandwidth	16, 100 KHz	
	End scale value	±20 mv~±20 V	
	Distortion factor	<0.5%	

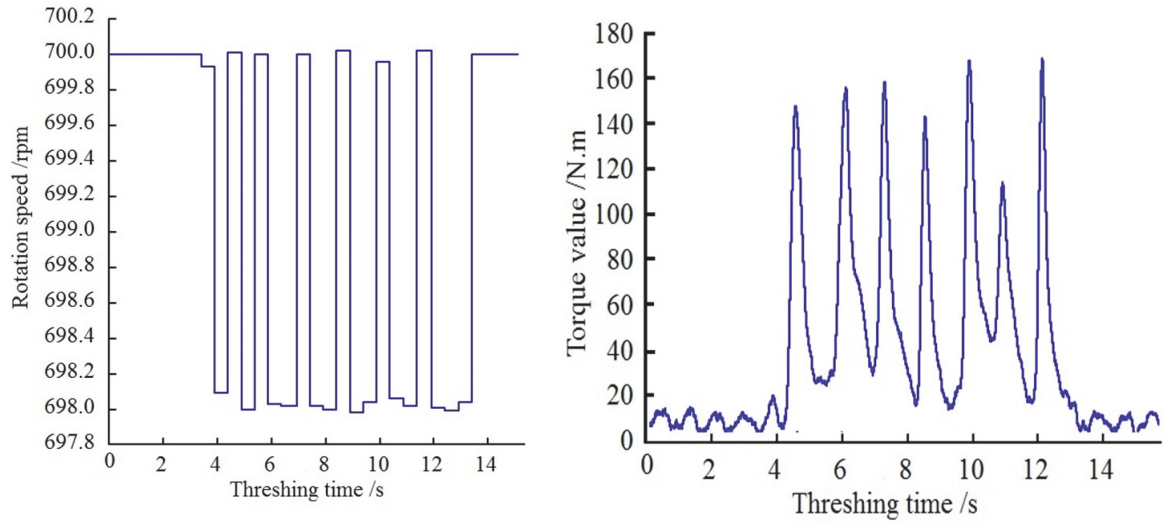

(a) Rotation speed along threshing time

(b) Torque signal along threshing time

Figure 7: Curves of torque and speed state of tangential threshing cylinder during rice threshing process.

3. Results and Discussion

3.1. Torque and Speed State of Threshing Cylinder. During the rice threshing process, the rotation speed of tangential threshing cylinder was tested and recorded by HAD-CYB-803S torque-speed sensors. The rotation speed curves of tangential threshing cylinder were shown in Figure 7(a). The torque signal of tangential threshing cylinder was shown in Figure 7(b).

As shown in Figure 7(a), the starting state rotation speed was 700 rpm. But the actual rotation speed was 698.1 rpm during rice threshing process. Rotation speed was fluctuated within the range of 0~3 rpm. Tang et al. also have tested the threshing cylinder torque and rotation [27]. There were the same conclusions. So rotation speed frequency was the minor fluctuation. The start state rotation speed frequency was 11.67 Hz (rotation speed 700 rpm). During rice threshing process, the rotation speed frequency was 11.64 Hz (rotation speed 698.1 rpm). There was a rotation speed fluctuation frequency during the rice threshing. As shown in Figure 7(a), there were seven times up and down fluctuations. The time intervals of up and down fluctuations were 0.4 s, 0.8 s, and 1.2 s. The up and down fluctuations frequency were 2.50 Hz, 1.25 Hz, and 0.83 Hz. As shown in Figure 7(b), there were also up and down fluctuations in the threshing torque value. As shown in Figure 7, the up and down fluctuations frequencies of threshing torque were the same as the rotation speed. Rotation speed fluctuations were caused by threshing torque fluctuations. A similar decrease in rotation speed was observed by Alizadeh and Khodabakhshipour [28]. The rice threshing process itself was the cause of decrease in rotation speed and load of rice threshing. There was incentive frequency in rice threshing process, which could induce cylinder vibration or cause resonance phenomenon.

3.2. Restricted and Working Modalities of Threshing Cylinder. Because the tangential threshing cylinder was mounted on the rolling bearing seat, the cylindrical surface at both ends of the drive shaft was applied to restrict the cylinder shaft. Then the axial and radial freedom were limited. The tangential threshing cylinder can rotate but cannot move axially. The modal shapes under restricted modality were solved by ANSYS Workbench, which were shown in Figure 8. The 1st modal shapes' frequency was 44.6 Hz, shown in Figure 8(a). The 2nd modal shapes' frequency was 94.9 Hz, shown in Figure 8(b). The 3rd modal shapes' frequency was 157.1 Hz, shown in Figure 8(c).

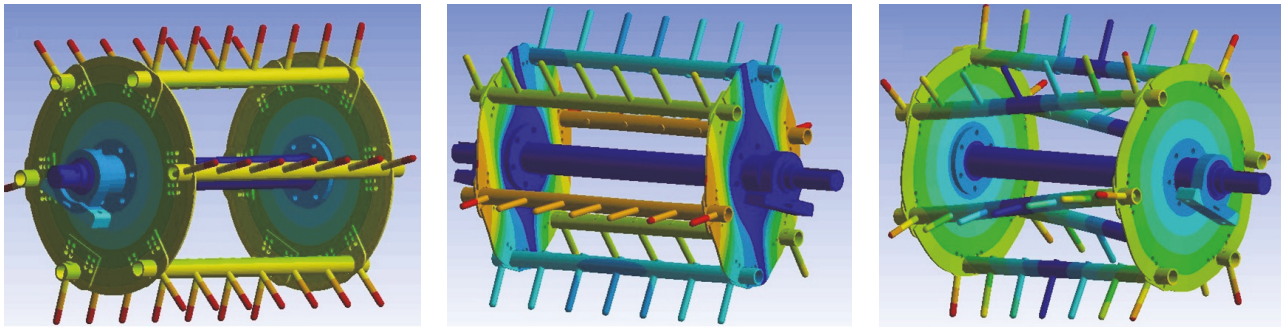

(a) 1st modal shapes (b) 2nd modal shapes (c) 3rd modal shapes

Figure 8: Modal shapes under restricted modality.

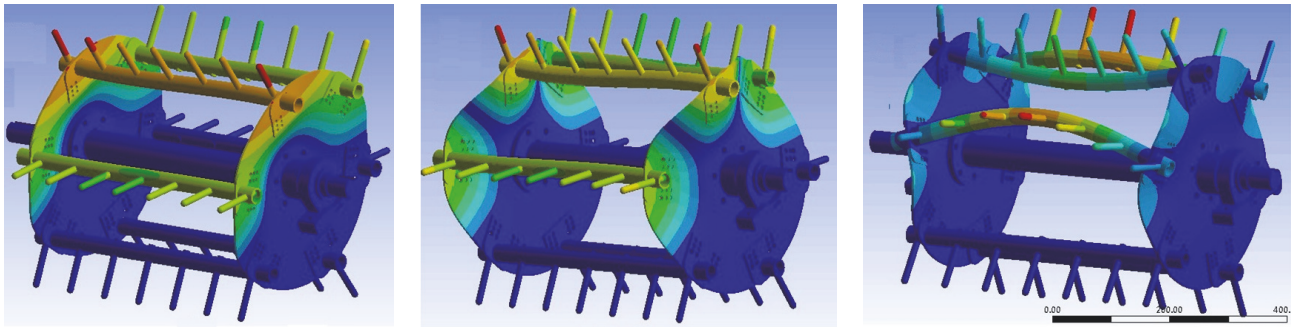

(a) 1st modal shapes (b) 2nd modal shapes (c) 3rd modal shapes

Figure 9: Modal shapes of working modality.

According to Figure 8, the 1st intrinsic constraint frequency was 44.6 Hz, which was higher than the rotation speed frequency 11.66 Hz and threshing speed frequency 11.63 Hz. Intrinsic constraint frequencies were higher than the incentive frequency during the rice threshing process, with the same results as the 2nd and 3rd modal shapes' frequency of restricted modality.

The modal shapes of working modality were shown in Figure 9. The 1st, 2nd, and 3rd modal shapes' frequency were 68.9 Hz, 107.4 Hz, and 171.2 Hz, respectively. The 3 kinds of mode shapes were, respectively, shown in Figures 9(a), 9(b), and 9(c).

According to Figure 9, the 1st, 2nd, and 3rd modal shapes' frequencies were higher than the rotation speed frequency and threshing speed frequency. The threshing torque fluctuations and rotation speed fluctuations were caused by rice threshing process. But these up and down fluctuations frequency were 2.5 Hz, 1.25 Hz, and 0.83 Hz. So the up and down fluctuation frequency was smaller than the 1st, 2nd, and 3rd intrinsic constraint frequency. When the excitation frequency is less than the intrinsic frequency, resonance does not occur. This criterion is widely used to determine whether resonance phenomena occur or not [29, 30]. This rotation speed frequency of tangential threshing cylinder would not induce the occurrence of resonance phenomenon during rice threshing process.

3.3. Vibration and Frequency State of Threshing Cylinder. The tangential threshing cylinders were consisting of cylinder shaft, threshing bars, and connectivity spokes. Because these parts were a whole structure, the shaft vibration could represent the tangential threshing cylinders vibration. Then cylinder shaft vibration amplitude and frequency can be used to evaluate the vibration state of tangential threshing cylinder. Bearing seat of shaft vibration amplitude and frequency used to reveal the vibration state of rotor were confirmed and applied by Ferfecki et al. [31].

3.3.1. Time-Domain Vibration of Threshing Cylinder. During the rice threshing process, the bearing seat vibration was measured by acceleration sensors. The vibration signal of bearing seat was recorded as time-domain process [32, 33]. There were two states of tangential threshing cylinder, respectively, idling state of no-load and load state of rice threshing process. The vibration signals of idling state of no-load were shown in Figure 10. The X direction vibration signal represented the feed straw flow direction (front and back direction), shown in Figure 10(a). The Y direction vibration signal represented the cylinder axis (left and right direction), shown in Figure 10(b). The Z direction vibration signal represented the cylinder axis (up and down direction), shown in Figure 10(c).

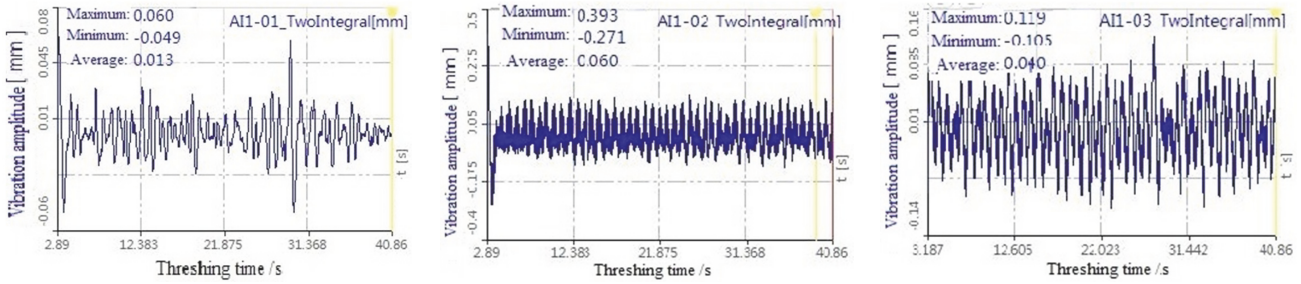

(a) X direction (b) Y direction (c) Z direction

Figure 10: Time-domain vibration signal of no-load cylinder rotation.

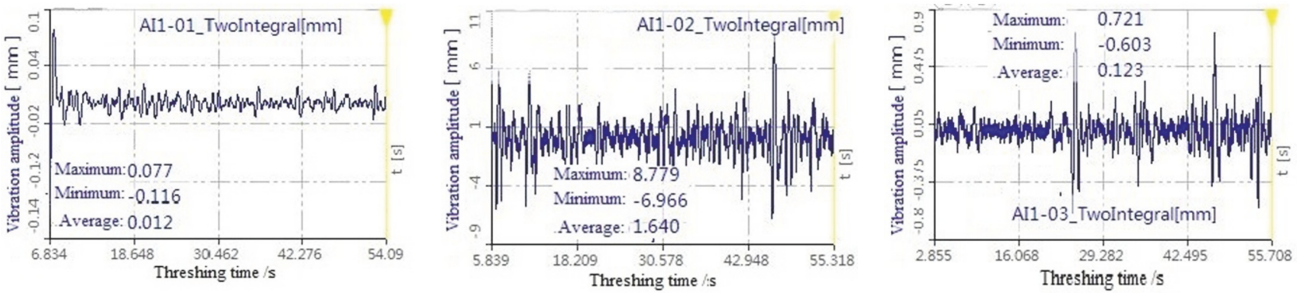

(a) X direction (b) Y direction (c) Z direction

Figure 11: Time-domain vibration signal of rice threshing process.

The vibration signal of load state of rice threshing process was shown in Figure 11. The X, Y, and Z direction represented the same state as the idling state of no-load.

According to Figures 10(a) and 11(a), when the tangential threshing cylinder was in idling state of no-load, the vibration amplitude of X direction (front and back direction of straw flow feeding) was −0.049~0.060 mm, and the average vibration amplitude was 0.013 mm. This vibration state of X direction was balanced, and the vibrational state could be negligible. But when rice flow was feeding into tangential threshing cylinder, the vibration amplitude of X direction was slightly increased. The vibration amplitude of X direction load state of rice threshing process was −0.012~0.077 mm; the average vibration amplitude was 0.012 mm.

According to Figures 10(b) and 11(b), the vibration amplitude was obviously increased in Y direction (left and right direction). The vibration amplitudes of idling state of no-load and load state of rice threshing process were −0.271~0.393 and −6.966~8.779 mm. There were 22~25 times increases. The average vibration amplitude of rice threshing process was 1.640 mm. Based on the vibration amplitude statistics, the average value 1.64 mm reflected load state of rice threshing process with random vibration [34]. Average vibration amplitude of rice threshing process changed as times changed. These left and right directions along shaft vibration amplitude were induced by the straw flow axial movement. The threshing bars were not uniform and have exactly the same position on the cylinder. In order to clarify their vibration characteristics and verify the validity of the analysis, a dynamic model for agricultural rubber crawler vehicles equipped with movable track rollers was constructed by Mitsuoka et al., indicating that the vibration characteristics were different, although the location arrangements were similar [17].

According to Figures 10(c) and 11(c), the vibration amplitude was slightly increased in Z direction (up and down direction). The vibration amplitudes of idling state of no-load and load state of rice threshing process were −0.105~0.119 and −0.603~0.721 mm. Average vibration amplitudes of idling state of no-load and load state of rice threshing process were 0.04 mm and 0.123 mm. This vibrational state could be ignored.

According to Figures 10 and 11, vibration amplitude of X direction and Z direction was slightly increased during the rice threshing process. The vibrational state could be ignored. But the vibration amplitude was obviously increased in Y direction. Vibration amplitude of load state of rice threshing process was with random vibration. Chen et al. tested the vibration of the 4LZ-2 combine harvester on the location of the driver room, which indicated that most vibration intensity under the bad working condition was 4.26 mm [35].

3.3.2. Frequency Domain Vibration of Threshing Cylinder. Based on the time-domain vibration signal of tangential threshing cylinders with idling state of no-load and load state of rice threshing process, the frequency domain vibration could be obtained. Frequency domain vibration signal of no-load cylinder rotation was shown in Figure 12.

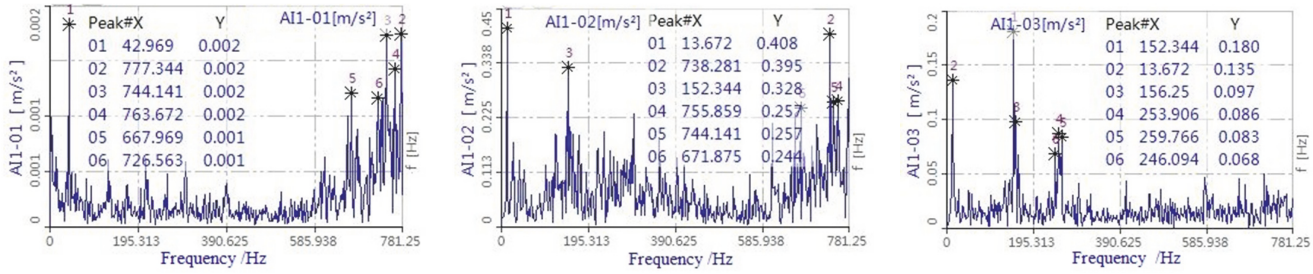

(a) X direction (b) Y direction (c) Z direction

Figure 12: Frequency domain vibration signal of no-load cylinder rotation.

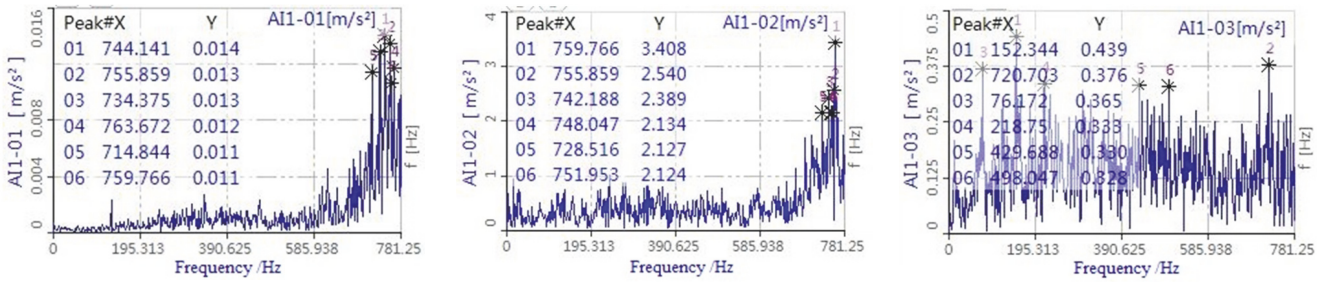

(a) X direction (b) Y direction (c) Z direction

Figure 13: Frequency domain vibration signal of rice threshing process.

According to Figure 12, when the tangential threshing cylinder was with no-load cylinder rotation, there was a low-frequency vibration frequency with larger contribution to the vibration amplitude at X, Y, and Z direction. At the X direction vibration amplitude, the vibration frequency 42.969 Hz was larger contribution. In the Y and Z directions' vibration amplitude, the larger contribution vibration frequency was 13.672 Hz.

In the same way, frequency domain vibration signal of rice threshing process was shown in Figure 13. The one to six modals which had larger contribution to the vibration amplitude were recorded and shown in the figures. Other modal frequencies could also be obtained from these figures.

According to Figure 13, when the tangential threshing cylinder was in load state of rice threshing process, the vibration frequency which was larger contribution to the vibration amplitude was obviously increased. At X and Y direction, the minimum frequency was higher than 740 Hz. This high frequency is impossible to resonate. But in the Z direction, the 76.12 Hz and 152.344 Hz were lower frequencies while another frequency was higher than 200 Hz. There were also some low-frequency vibration frequencies, but they had lesser contribution to the vibration amplitude.

3.4. Shaft Vibration and Axis Trajectory of Threshing Cylinder. Axis trajectory was an important part of the rotor vibration signal. It was composed of two mutually perpendicular vibration signals on the same section of the shaft. The dynamic characteristics and shape of the shaft trajectory contained a lot of fault information, which could reflect the operation of the equipment visual and intuitive status.

In order to analyze the shaft vibration and axis trajectory of tangential threshing cylinders, vibration waveform was extracted from time-domain vibration signal. Vibration signals of idling state of no-load and load state of rice threshing process were extracted and used to analyze shaft vibration and the axis trajectory.

3.4.1. Shaft Vibration and Variation of Threshing Cylinder. Based on the time-domain vibration signal of tangential threshing cylinders, the idling state of no-load and load state of rice threshing process were given. Because the X direction represented the feed straw flow direction and the Z direction represented the cylinder axis, a typical vibration waveform was obtained and shown in Figure 14.

Based on the time-domain vibration signal of tangential threshing cylinders with load state of rice threshing process, a typical vibration waveform was obtained and shown in Figure 15.

According to Figures 14 and 15, vibration waveform of X direction was a certain periodicity. Vibration amplitude was changing as rotation time. Because the rotation speed of tangential threshing cylinder was 700 rpm, the rotation cycle time was 0.086 s. As shown in Figure 14, every fluctuation period (a complete crest and trough) was about 0.7 s. The fluctuation period of no-load cylinder rotation was 8 times as long as the rotation cycle time. During the rice threshing process, the fluctuation period was 0.8 s, which was about 10 times as long as the rotation cycle time.

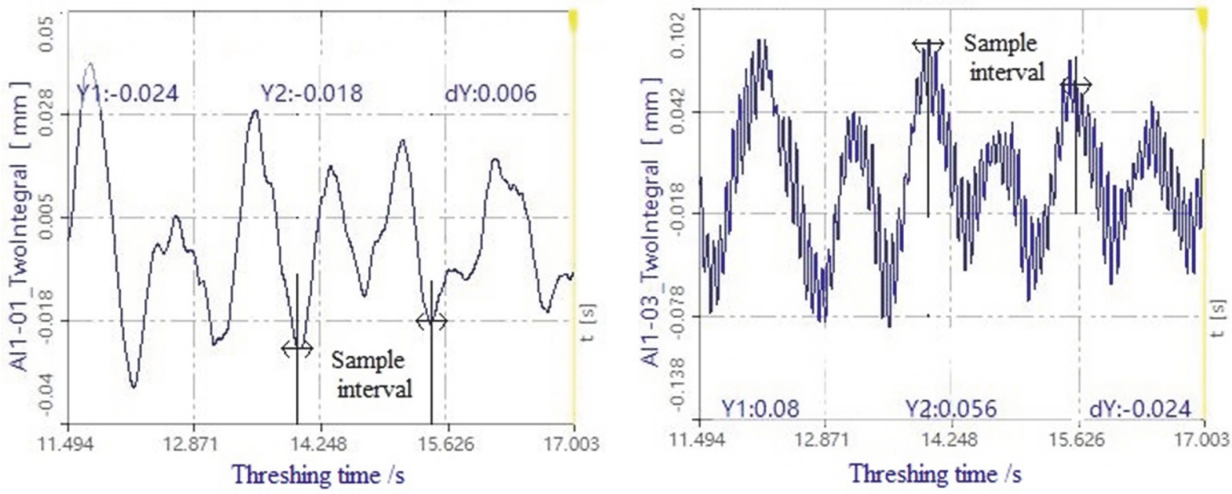

(a) X direction (b) Z direction

Figure 14: Typical vibration waveform of no-load cylinder rotation.

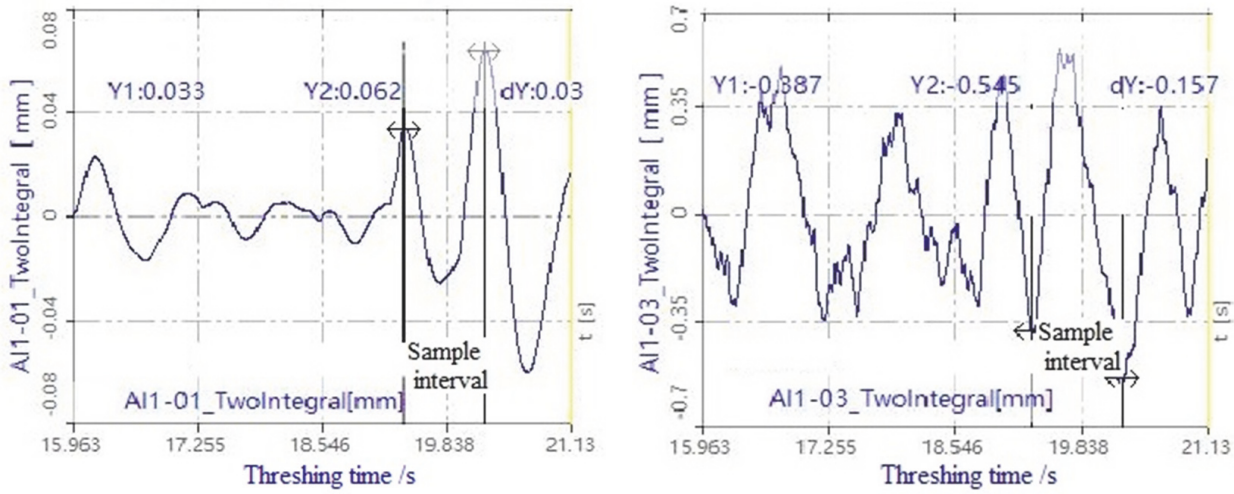

(a) X direction (b) Z direction

Figure 15: Typical vibration waveform of rice threshing process.

3.4.2. Axis Trajectory and Variation of Threshing Cylinder. Based on the typical vibration waveform shown in Figure 14, vibration amplitude values of double fluctuation period were exported from the time-domain vibration signal. The sample interval values of X and Z direction vibration waveform of no-load cylinder rotation were shown in Table 2. Based on the vibration amplitude values of X and Z direction, the vibration amplitude and vibration phase were calculated and shown in Table 2.

As shown in Figure 14(b), the vibration waveform of Z direction was compound curve. There was small vibration cycle on the large fluctuation period (fluctuation period was 0.7 s). Small cycle vibration amplitude values were exported from Z direction small vibration cycle. The results of vibration values of small vibration on up and down direction were shown in Table 3. Based on the vibration amplitude values of X and Z direction, the vibration amplitude and vibration phase were calculated and shown in Table 3.

Fukushima et al. proposed a trajectory constructed by the coordinates based on each frequency component in order to examine the vibration characteristics in detail. In addition, the part where the nonlinear vibration occurred was observed [36]. Based on the sample interval values of Tables 2 and 3, axis trajectory and variation of no-load cylinder rotation were drawn and shown in Figure 16.

According to Figure 16(a), the axis trajectories were mainly concentrated in two areas. In these two areas, X-axis and Z-axis coordinates have exactly the opposite value. These curves mean that the X and Z directions were opposite in phase. The vibration amplitude values were 0~87.14 um. This axis trajectory was random, but there was a concentrated area. As shown in Figure 16(b), the axis trajectory of small

Table 2: X and Z direction vibration values of no-load cylinder rotation.

Serial number	Cylinder threshing time/s	X direction vibration amplitude/um	Z direction vibration amplitude/um	Vibration amplitude/um	Vibration phase/°
1	14.00	−24	82	85	−73.69
2	14.05	−22	62	66	−70.46
3	14.10	−15	25	29	−59.04
4	14.15	−6	33	34	−79.69
5	14.20	2	40	40	87.14
6	14.25	9	−6	11	−33.69
7	14.30	13	−28	31	−65.10
8	14.35	16	−1	16	−3.58
9	14.40	14	−20	24	−55.01
10	14.45	9	−47	48	−79.16
11	14.50	2	−3	4	−56.31
12	14.55	−1	16	16	−86.42
13	14.60	−4	−7	8	60.25
14	14.65	−8	10	13	−51.34
15	14.70	−12	22	25	−61.39
16	14.75	−10	29	31	−70.97
17	14.80	−2	11	11	−79.69
18	14.85	0	−7	7	0.00
19	4.900	2	25	25	85.43
20	14.95	4	5	6	51.34
21	15.00	10	−52	53	−79.11
22	15.05	17	−39	43	−66.45
23	15.10	21	−24	32	−48.81
24	15.15	20	−55	59	−70.02
25	15.20	15	−47	49	−72.30
26	15.25	5	−14	15	−70.35
27	15.30	−5	−8	9	57.99
28	15.35	−14	−12	18	40.60
29	15.40	−17	20	26	−49.64

Note. Vibration amplitude was square root of X and Z direction vibration amplitude. Vibration phase was horizontal angle of vibration amplitude and X direction.

Table 3: X and Z direction vibration values of small vibration on up and down direction.

Serial number	Cylinder threshing time/s	X direction vibration amplitude/um	z direction vibration amplitude/um	Vibration amplitude/um	Vibration phase/°
1	33.61	31	46	55	56.02
2	33.62	36	37	52	45.78
3	33.63	41	16	44	21.32
4	33.64	45	7	46	8.84
5	33.65	49	11	50	12.65
6	33.66	52	26	58	26.56
7	33.67	54	43	69	38.53
8	33.68	57	53	78	42.92

Note. Vibration amplitude was square root of X and Z direction vibration amplitude. Vibration phase was horizontal angle of vibration amplitude and X direction.

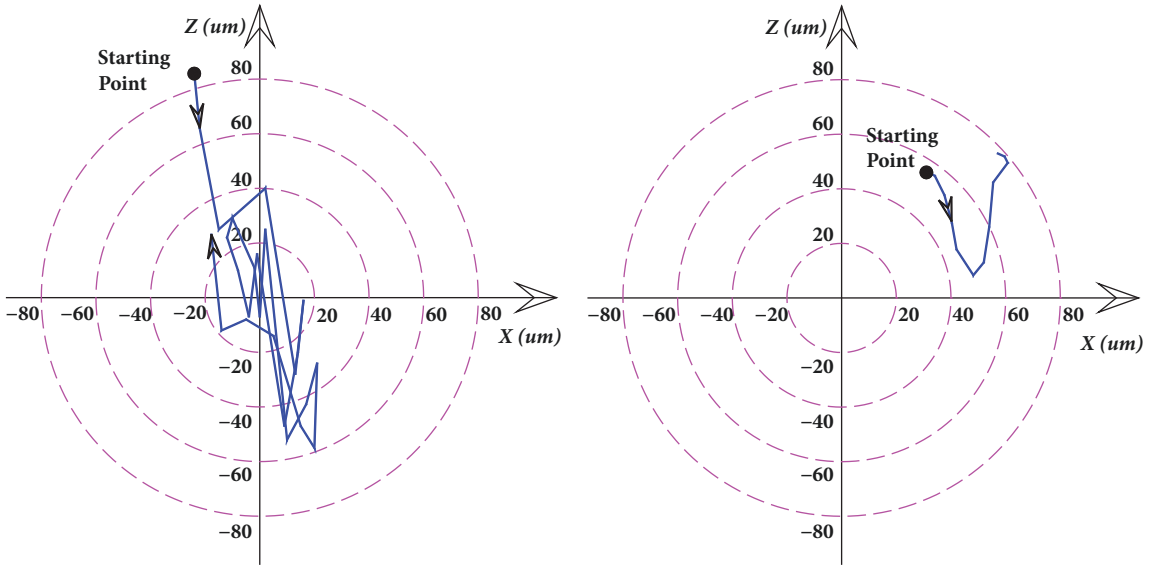

(a) Large vibration cycle of cylinder shaft

(b) Small vibration cycle of Z direction

Figure 16: Axis trajectory and variation of no-load cylinder rotation.

Table 4: X and Z direction vibration values of rice threshing process.

Serial number	Cylinder threshing time/s	X direction vibration amplitude/um	z direction vibration amplitude/um	Vibration amplitude/um	Vibration phase/°
1	19.40	32	−164	167	−78.96
2	19.45	26	37	45	54.90
3	19.50	14	191	192	85.81
4	19.55	1	404	404	89.86
5	19.60	−12	530	530	−88.70
6	19.65	−21	481	481	−87.50
7	19.70	−26	490	491	−86.96
8	19.75	−27	490	491	−86.85
9	19.80	−25	307	308	−85.34
10	19.85	−23	156	158	−81.61
11	19.90	−20	92	94	−77.73
12	19.95	−14	7	16	−26.56
13	20.00	4	−113	113	−87.97
14	20.05	22	−210	211	−84.02
15	20.10	40	−255	258	−81.08
16	20.15	56	−340	345	−80.65
17	20.20	62	−556	559	−83.64

Note. Vibration amplitude was square root of X and Z direction vibration amplitude. Vibration phase was horizontal angle of vibration amplitude and X direction.

cycle vibration was U-shaped. Due to the different variation of the vibration curves, the trend and phase of each trajectory were the same although the amplitude of each trajectory was different. The different vibration period curves were only the amplitude-to-scale relationship.

In the same way, the results of vibration amplitude values of rice threshing process were shown in Table 4. Based on the vibration amplitude values of X and Z direction, the vibration amplitude and vibration phase were calculated and shown in Table 4.

Based on the vibration amplitude values of rice threshing process shown in Table 4, axis trajectory and variation were drawn and shown in Figure 17.

According to Figure 17, the axis trajectories of rice threshing process were similar to that of no-load cylinder rotation. The axis trajectories were mainly concentrated in

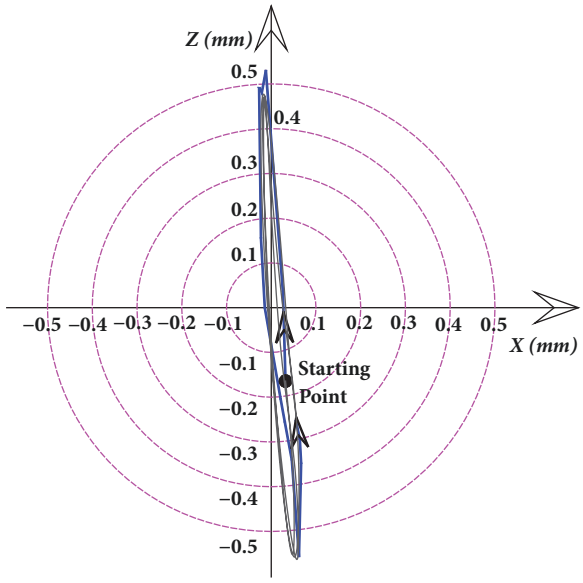

Figure 17: Axis trajectory and variation of rice threshing process.

two areas. These curves mean that the X and Z directions were opposite in phase. But the axis trajectories outline increased more than 6 times. The vibration amplitude values were 0~559 um. Therefore, the rice threshing process would induce an obvious vibration compared to that of no-load cylinder rotation.

The normal axis trajectory should be a stable ellipse with similar long and short axes. When the axis was not centered, the trajectory of the axis was crescent-shaped, banana-shaped, or "8"-shaped. When the rotating shaft was rubbed, many serrated corners and small rings appear in axis trajectory [6, 36]. As shown in Figure 16(a), there were many serrated corners which meant that the tangential threshing cylinder was restrained and rubbed by rice stems. If the repetitiveness of the shape and size of the axis trajectory were good, then the whirl of the rotor was stable; otherwise, it was unstable. When the rotor self-excited vibration occurs, its axial trajectory will be unstable; not only will the shape and size of the rotor change greatly, but also large loops and small loops will appear. As shown in Figure 17, axis has obvious jump phenomenon. The jump of tangential threshing cylinder axis was induced by the impact of uneven rice stalks on the barrel in the concave gap. This unbalanced vibration was induced by the rice stalks in the concave gap.

4. Conclusion

In this paper, the restricted and working modalities of tangential threshing cylinder were solved, and shaft vibration of tangential threshing cylinder at idling state of no-load and load state of rice threshing process were tested and analyzed. The main conclusion was shown as follows.

(1) During the rice threshing process, there was a rotation speed fluctuation frequency during rice threshing. The up and down fluctuations frequency were 2.5 Hz, 1.25 Hz, and 0.83 Hz. The working modality was solved by ANSYS Workbench, which showed that the 1st, 2nd, and 3rd modal shapes' frequency were 68.9 Hz, 107.4 Hz, and 171.2 Hz, respectively. The 1st, 2nd, and 3rd modal shapes' frequencies were higher than the rotation speed frequency 11.66 Hz and threshing speed frequency 11.63 Hz. This rotation speed frequency would not induce the occurrence of resonance phenomenon.

(2) When tangential threshing cylinder was in idling state of no-load, the vibration amplitude of front and back direction of straw flow feeding direction was −0.049~0.06 mm, and the average vibration amplitude was 0.013 mm. The vibration amplitude was obviously increased in left and right direction with rice straw flow feeding. The vibration amplitude of rice threshing process was −6.97~8.78 mm. There were 22~25 times increases. Based on the vibration amplitude statistics, the average value 1.64 mm reflected the load state of rice threshing process with random vibration.

(3) The trend and phase of each trajectory were the same although the amplitude of each trajectory was different. The different vibration period curves were only the amplitude-to-scale relationship. But the axis trajectories were mainly concentrated in two areas. The vibration amplitude values of rice threshing process were 0~559 um, which were obviously more than idling state of no-load. There were many serrated corners in the trajectory, which mean that the tangential threshing cylinder was restrained and rubbed by rice stems. The jump of tangential threshing cylinder axis was induced by the impact of uneven rice stalks on the barrel in the concave gap.

Data Availability

The data used to support the findings of this study are available from the corresponding author upon request.

Conflicts of Interest

The authors declare that they have no conflicts of interest.

Acknowledgments

This research work was supported by the Natural Science Foundation of Jiangsu Province (BK20170553), National Natural Science Foundation of China (51705212), China Postdoctoral Science Foundation fund (2015M581742), Jiangsu Province Post-Doctoral Research Aid Program (1501111B), and a project funded by the Priority Academic Program Development of Jiangsu Higher Education Institutions (PAPD).

References

[1] P. I. Miu and H.-D. Kutzbach, "Modeling and simulation of grain threshing and separation in threshing units-Part I," *Computers and Electronics in Agriculture*, vol. 60, no. 1, pp. 96–104, 2008.

[2] Q. W. Chen, Z. D. Han, and J. W. Cui, "Development state and trend current situation of self-propelled combine harvester,"

Journal of Agricultural Science and Technology, vol. 17, no. 1, pp. 109–114, 2015.

[3] I. Hostens and H. Ramon, "Descriptive analysis of combine cabin vibrations and their effect on the human body," *Journal of Sound and Vibration*, vol. 266, no. 3, pp. 453–464, 2003.

[4] Y. C. Yao, Z. H. Song, Y. F. Du, X. Y. Zhao, E. R. Mao, and F. Liu, "Analysis of vibration characteristics and its major influenced factors of header for corn combine harvesting machine," *Transactions of the Chinese Society of Agricultural Engineering*, vol. 33, no. 13, pp. 40–49, 2017.

[5] W. Tomczyk and Z. Kowalczyk, "The wear processes in the aspect of construction quality and the need to apply agricultural machines servicing," *Journal of Research and Applications in Agricultural Engineering*, vol. 61, no. 2, pp. 114–119, 2016.

[6] T. Fukushima, E. Inoue, M. Mitsuoka, T. Okayasu, and K. Sato, "Collision vibration characteristics with interspace in knife driving system of combine harvester," *Engineering in Agriculture, Environment and Food*, vol. 5, no. 3, pp. 115–120, 2012.

[7] S. Chuan-Udom, "Development of a cutter bar driver for reduction of vibration for a rice combine harvester," *Asia-Pacific Journal of Science and Technology*, vol. 15, no. 7, pp. 572–580, 2017.

[8] Z. P. Gao, L. Z. Xu, Y. M. Li, Y. D. Wang, and P. P. Sun, "Vibration measure and analysis of crawler-type rice and wheat combine harvester in field harvesting condition," *Transactions of the Chinese Society of Agricultural Engineering*, vol. 33, no. 20, pp. 48–55, 2017.

[9] O. A. Polushkin, O. O. Polushkin, and I. M. Fofana, "More efficient balancing of rotors," *Russian Engineering Research*, vol. 37, no. 7, pp. 574–578, 2017.

[10] Y. S. Zhou, J. Zhang, X. Li, J. R. Yue, G. B. Xia, and W. Z. Yang, "Modal analysis of rasp bar type roller based on ANSYS-Workbench," *Agricultural Science & Technology and Equipment*, vol. 261, no. 3, pp. 25–27, 2016.

[11] J. Zapomel, P. Ferfecki, and P. Forte, "Analysis of the steady state unbalances response of rigid rotors on magnetorheological dampers: stability, force trans-mission and energy dissipation," *International Journal of Applied Mechanic*, vol. 6, no. 3, pp. 97–102, 2014.

[12] B. Bai and L. X. Zhang, "Dynamic response of hydro-turbine set shaft system under stochastic hydraulic excitation," *Journal of Drainage and Irrigation Machinery Engineering*, vol. 35, no. 5, pp. 398–423, 2017.

[13] S. Zhang and Z. Zhang, "Research on the field dynamic balance technologies for large diesel engine crankshaft system," *Shock and Vibration*, vol. 2017, Article ID 7150472, 10 pages, 2017.

[14] N. Wang, B. Hung, and Q. Wu, "Experiment and numerical simulation of vibration characteristics of hydrofoil in cavitating flow," *Journal of Drainage and Irrigation Machinery Engineering*, vol. 34, no. 4, pp. 321–327, 2016.

[15] B. Çakmak, T. Saraçoğlu, F. N. Alayunt, and C. Özarslan, "Vibration and noise characteristics of flap type olive harvesters," *Applied Ergonomics*, vol. 42, no. 3, pp. 397–402, 2011.

[16] J. H. Xie, X. K. Zhang, F. W. Zhang, T. Zhang, and F. Dai, "Modal analysis for threshing cylinder and topological optimization for cylinder axis based on Ansys-workbench," *Journal of Gansu Agricultural University*, vol. 51, no. 6, pp. 134–138, 2016.

[17] M. Mitsuoka, S. Inaba, E. Inoue et al., "Prediction and evaluation of vibration characteristics of an agricultural rubber crawler vehicle equipped with movable track rollers," *Journal of the Japanese Society of Agricultural Machinery*, vol. 70, no. 5, pp. 41–47, 2008.

[18] N. Hagiwara, S. Sakata, M. Takayanagi, K. Kikuchi, and I. Gyobu, "Analysis of coupled vibration response in a rotating flexible shaft-impeller system," *Journal of Mechanical Design*, vol. 102, no. 1, pp. 162–167, 1980.

[19] R. Ebrahimi, M. Esfahanian, and S. Ziaei-Rad, "Vibration modeling and modification of cutting platform in a harvest combine by means of operational modal analysis (OMA)," *Measurement*, vol. 46, no. 10, pp. 3959–3967, 2013.

[20] J. B. Krolczyk, S. Legutko, and G. M. Krolczyk, "Dynamic balancing of the threshing drum in combine harvesters-the process, Sources of imbalance and negative impact of mechanical vibrations," *Applied Mechanics and Materials*, vol. 69, no. 3, pp. 424–429, 2014.

[21] Z. Tang, Y. M. Li, Z. Zhao, and T. Sun, "Structural and parameter design of transverse multi-cylinders device on rice agronomic characteristics," *Spanish Journal of Agricultural Research*, vol. 13, no. 4, article e0216, p. 12, 2015.

[22] Y. C. Yao, Y. F. Du, Z. X. Zhu, E. R. Mao, and Z. H. Song, "Vibration characteristics analysis and optimization of corn combine harvester frame using modal analysis method," *Transactions of the Chinese Society of Agricultural Engineering*, vol. 31, no. 19, pp. 46–53, 2015.

[23] D. Tan, Q. Wang, and Y. Wu, "Modal analysis of in-wheel motor-driven electric vehicle based on bond graph theory," *Shock and Vibration*, vol. 2017, Article ID 6459154, 9 pages, 2017.

[24] M. Bermejo, A. P. Santos, and J. M. Goicolea, "Development of practical finite element models for collapse of reinforced concrete structures and experimental validation," *Shock and Vibration*, vol. 2017, Article ID 4636381, 9 pages, 2017.

[25] X. X. Xiao, H. Li, X. D. Qi, and M. Wang, "Modal and transient analysis of threshing cylinder based on ANSYS workbench," *Journal of Agricultural Mechanization Research*, vol. 2016, no. 8, pp. 46–50, 2016.

[26] Z. Tang, Y. M. Li, J. B. Liu, H. Zhang, and Y. W. Li, "Dynamic vibration test and analysis of 4LZ-2.5B combine harvester cutting table rack in wheat harvesting," *The International Agricultural Engineering Journal*, vol. 26, no. 1, pp. 79–86, 2017.

[27] Z. Tang, Y. M. Li, R. Wang, and J. S. Chen, "Experimental study of multi-source dynamic load of combine harvester in rice harvesting," *The International Agricultural Engineering Journal*, vol. 25, no. 3, pp. 46–52, 2016.

[28] M. R. Alizadeh and M. Khodabakhshipour, "Effect of threshing drum speed and crop moisture on the paddy grain damage in axial-flow thresher," *Cercetari Agronomice in Moldova*, vol. 43, no. 4, pp. 5–11, 2010.

[29] M. Ouisse and E. Foltête, "Model correlation and identification of experimental reduced models in vibroacoustical modal analysis," *Journal of Sound and Vibration*, vol. 342, pp. 200–217, 2015.

[30] J. Chou, B. J. Zhao, and Y. F. Zhao, "Impact of tongue angles on hydraulic and structural performance of double-channel pump based on fluid-structure interaction," *Journal of Drainage and Irrigation Machinery Engineering*, vol. 35, no. 5, pp. 496–503, 2016.

[31] P. Ferfecki, J. Zapoměl, and J. Kozánek, "Analysis of the vibration attenuation of rotors supported by magnetorheological squeeze film dampers as a multiphysical finite element problem," *Advances in Engineering Software*, vol. 104, no. 1, pp. 1–11, 2017.

[32] G. X. Ma, D. Y. Chen, and Y. S. Wan, "Vibration test of a self-moving grain combine harvester," *Modern Machinery*, vol. 2008, no. 2, pp. 59–61, 2008.

[33] W. Weijtjens, J. Lataire, C. Devriendt, and P. Guillaume, "Dealing with periodical loads and harmonics in operational modal analysis using time-varying transmissibility functions," *Mechanical Systems and Signal Processing*, vol. 49, no. 1-2, pp. 154–164, 2014.

[34] H. Risius, J. Hahn, M. Huth, R. Tölle, and H. Korte, "In-line estimation of falling number using near-infrared diffuse reflectance spectroscopy on a combine harvester," *Precision Agriculture*, vol. 16, no. 3, pp. 261–274, 2015.

[35] D. Y. Chen, K. Li, H. T. Li, and Y. F. Cheng, "The vibration test of combine harvester and the anti-vibration study of the monitor," in *Proceedings of the International Conference on Electrical and Control Engineering (ICECE '10)*, pp. 4466–4469, Wuhan, China, June 2010.

[36] T. Fukushima, E. Inoue, M. Mitsuoka, M. Matsui, and T. Okayasu, "Vibration characteristics and modeling of knife driving system of combine harvester (part 2)," *Journal of the Japanese Society of Agricultural Machinery*, vol. 68, no. 5, pp. 59–64, 2006.